Inorganic Chemistry
Article

Inorg. Chem. **2010**, *49*, 2901–2910 **2901**
DOI: 10.1021/ic902439x

One- and Two-Electron-Transfer Reactions of (dpp-Bian)Sm(dme)$_3$

Igor L. Fedushkin,*,† Olga V. Maslova,† Markus Hummert,‡ and Herbert Schumann§,⊥

†*G. A. Razuvaev Institute of Organometallic Chemistry, Russian Academy of Sciences, Tropinina 49, Nizhny Novgorod 603600, Russia,* ‡*Institut für Angewandte Photophysik, Technische Universität Dresden, George-Bähr-Strasse 1, Dresden 01062, Germany, and* §*Institut für Chemie, Technische Universität Berlin, Strasse des 17. Juni 135, Berlin 10623, Germany.* ⊥*Deceased on January 12, 2010.*

Received December 8, 2009

The reduction of 1,2-bis[(2,6-diisopropylphenyl)imino]acenaphthene (dpp-Bian) with an excess of samarium in 1,2-dimethoxyethane (dme) affords the Sm^{II} complex (dpp-Bian)Sm(dme)$_3$ (**1**). The reaction of **1** with 0.5 mol equiv of 1,2-dibromostilbene proceeds with the formation of the dimeric Sm^{III} complex [(dpp-Bian)SmBr(dme)]$_2$ (**2**). Oxidation of both the metal and the dpp-Bian ligand takes place if **1** is reacted with equimolar amounts of 1,2-dibromostilbene or iodine, yielding the monomeric Sm^{III} derivatives (dpp-Bian)SmBr$_2$(dme) (**3**) and (dpp-Bian)SmI$_2$(THF)$_2$ (**4**; THF = tetrahydrofuran), respectively. The reaction of **1** with 0.5 mol equiv of iodine followed by 0.5 mol equiv of tetramethylthiuram disulfide gives the Sm^{III} complex (dpp-Bian)SmI[SC(S)NMe$_2$](dme) (**5**). Compound **4** and *t*BuOK react with the formation of the iodine-bridged dimer [(dpp-Bian)SmI(O*t*Bu)(THF)]$_2$ (**6**). Complexes **1** and **2** have been characterized by ^{1}H NMR spectroscopy and complexes **2**−**6** by their molecular structures, which were determined by single-crystal X-ray diffraction.

Introduction

Acenaphthene-1,2-diimines (Bians) proved to be versatile ligands in coordination chemistry. They were used as ligands in transition-metal complexes for the first time by members of the research groups around Elsevier, Coates, and Brookhart in the early 1990s. Up to now, a great number of transition-metal complexes with neutral Bian ligands have been reported that serve well as catalysts in organic reactions, especially in the polymerization of α-olefins.[1−7] In 2003, we demonstrated the ability of 1,2-bis[(2,6-diisopropylphenyl)-imino]acenaphthene (dpp-Bian) to act as an "electron sponge". Thus, the reduction of dpp-Bian with sodium resulted in the formation of its mono-, di-, tri-, and tetra-anions, respectively.[8] The redox activity of dpp-Bian has been further documented by the preparation of a series of group II[9] and XIII[10] metal complexes with radical-anionic

*To whom correspondence should be addressed. E-mail: igorfed@iomc.ras.ru. Phone: +7 831 4629631.

(1) van Laren, M. W.; Elsevier, C. J. *Angew. Chem., Int. Ed.* **1999**, *38*, 3715–3717.
(2) (a) van Belzen, R.; Hoffmann, H.; Elsevier, C. J. *Angew. Chem., Int. Ed. Engl.* **1997**, *36*, 1743–1745. (b) Grasa, G. A.; Singh, R.; Stevens, E. D.; Nolan, S. P. *J. Organomet. Chem.* **2003**, *687*, 269–279.
(3) Heumann, A.; Giordano, L.; Tenaglia, A. *Tetrahedron Lett.* **2003**, *44*, 1515–1518.
(4) (a) Cherian, A. E.; Lobkovsky, E. B.; Coates, G. W. *Chem. Commun.* **2003**, *20*, 2566–2567. (b) Al-Abaidi, F.; Ye, Z.; Zhu, S. *Macromol. Chem. Phys.* **2003**, *204*, 1653–1659. (c) Fassina, V.; Ramminger, C.; Seferin, M.; Mauler, R. S.; de Souza, R. F.; Monteiro, A. L. *Macromol. Rapid Commun.* **2003**, *24*, 667–670. (d) Leatherman, M. D.; Svejda, S. A.; Johnson, L. K.; Brookhart, M. *J. Am. Chem. Soc.* **2003**, *125*, 3068–3081. (e) Ivanchev, S. S.; Tolstikov, G. A.; Badaev, V. K.; Ivancheva, N. I.; Oleinik, I. I.; Khaikin, S. Ya.; Oleinik, I. V. *Vysokomol. Soedin., Ser. A, B* **2002**, *44*, 1478−1483 [*Polym. Sci. USSR, Ser. A, B* **2002**, *44*, 931−936 (English translation)]. (f) Killian, C. M.; Tempel, D. J.; Johnson, L. K.; Brookhart, M. *J. Am. Chem. Soc.* **1996**, *118*, 11664–11665. (g) Pellecchia, C.; Zambelli, A.; Mazzeo, M.; Pappalardo, D. *J. Mol. Catal. A: Chem.* **1998**, *128*, 229–237. (h) Cherian, A. E.; Rose, J. M.; Lobkovsky, E. B.; Coates, G. W. *J. Am. Chem. Soc.* **2005**, *127*, 13770–13771. (i) Rose, J. M.; Cherian, A. E.; Coates, G. W. *J. Am. Chem. Soc.* **2006**, *128*, 4186–4187.
(5) Kim, I.; Hwang, J. M.; Lee, J. K.; Ha, C. S.; Woo, S. I. *Macromol. Rapid Commun.* **2003**, *24*, 508–511.
(6) Johnson, L. K.; Killian, C. M.; Brookhart, M. *J. Am. Chem. Soc.* **1995**, *117*, 6414–6415.
(7) Alonso, J. C.; Neves, P.; da Silva, M. J. P.; Quintal, S.; Vaz, P. D.; Silva, C.; Valente, A. A.; Ferreira, P.; Calhorda, M. J.; Felix, V.; Drew, M. G. B. *Organometallics* **2007**, *26*, 5548–5556.
(8) Fedushkin, I. L.; Skatova, A. A.; Chudakova, V. A.; Fukin, G. K. *Angew. Chem., Int. Ed.* **2003**, *42*, 3294–3298.
(9) (a) Fedushkin, I. L.; Skatova, A. A.; Chudakova, V. A.; Fukin, G. K.; Dechert, S.; Schumann, H. *Eur. J. Inorg. Chem.* **2003**, 3336–3346. (b) Fedushkin, I. L.; Khvoinova, N. M.; Skatova, A. A.; Fukin, G. K. *Angew. Chem., Int. Ed.* **2003**, *42*, 5223–5226. (c) Fedushkin, I. L.; Skatova, A. A.; Cherkasov, V. K.; Chudakova, V. A.; Dechert, S.; Hummert, M.; Schumann, H. *Chem.—Eur. J.* **2003**, *9*, 5778–5783. (d) Fedushkin, I. L.; Morozov, A. G.; Rassadin, O. V.; Fukin, G. K. *Chem.—Eur. J.* **2005**, *11*, 5749–5757. (e) Fedushkin, I. L.; Makarov, V. M.; Rosenthal, E. C. E.; Fukin, G. K. *Eur. J. Inorg. Chem.* **2006**, 827–832. (f) Fedushkin, I. L.; Morozov, A. G.; Hummert, M.; Schumann, H. *Eur. J. Inorg. Chem.* **2008**, 1584–1588.
(10) (a) Schumann, H.; Hummert, M.; Lukoyanov, A. N.; Fedushkin, I. L. *Organometallics* **2005**, *24*, 3891–3896. (b) Lukoyanov, A. N.; Fedushkin, I. L.; Schumann, H.; Hummert, M. *Z. Anorg. Allg. Chem.* **2006**, *632*, 1471–1476. (c) Lukoyanov, A. N.; Fedushkin, I. L.; Hummert, M.; Schumann, H. *Russ. Chem. Bull.* **2006**, *55*, 422–428. (d) Schumann, H.; Hummert, M.; Lukoyanov, A. N.; Fedushkin, I. L. *Chem.—Eur. J.* **2007**, *13*, 4216–4222. (e) Fedushkin, I. L.; Lukoyanov, A. N.; Hummert, M.; Schumann, H. *Russ. Chem. Bull.* **2007**, *56*, 1765–1770.

Published on Web 02/12/2010

Chart 1

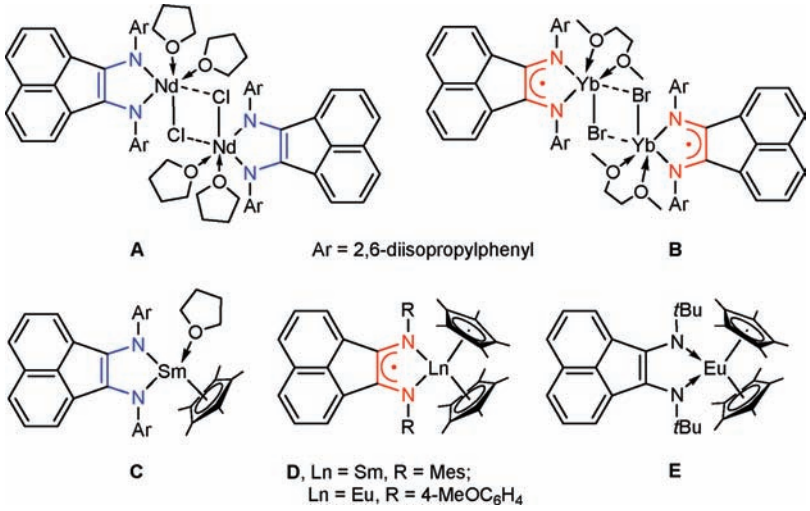

and dianionic dpp-Bian ligands. Moreover, the electronic and spatial feature of the dpp-Bian ligand allowed the isolation of molecular species with direct Zn−Zn,[11] Ga−Ga,[12] Zn−Ga,[12] Li−Ga[13] and Na−Ga[13] bonds. A review concerning this development of the coordination chemistry of Bian ligands with s- and p-block elements was published very recently.[14] By comparison, lanthanide complexes with Bian ligands have been studied much less and are limited to those presented in Chart 1 showing the structures **A**,[15] **B**,[16] and **C**−**E**, respectively.[17]

One of our particular interests concerns the use of metal complexes formed from redox-active ligands and redox-inactive metals like magnesium or aluminum in organic synthesis. In such systems, the metal is supposed to provide a coordination site for the organic substrate, which then may be reduced or oxidized by the metal-bonded ligand. Referring to this, the reactivity of dpp-Bian magnesium complexes is quite well studied. For instance, (dpp-Bian)$Mg(THF)_3$ (THF = tetrahydrofuran) readily reacts with oxidants like CuCl,[18] I_2,[18] Ph(Br)CHCH(Br)Ph,[18] TEMPO,[19] diphenyl ketone,[9c] or disulfides[20] to give the complexes (dpp-Bian)$MgOx(THF)_n$ (Ox = Cl^-, Br^-, I^-, $TEMPO^-$, $Ph_2CO^{\cdot-}$, RS^-), each of them containing the dpp-Bian ligand in its radical-anionic form. These oxidants may also withdraw two electrons from (dpp-Bian)$Mg(THF)_3$, but all of these reactions proceed with the release of the formed neutral ligand from the magnesium atom. However, recently, a two-electron oxidative process has been realized in the reaction of (dpp-Bian)Ga−Ga(dpp-Bian) with 2 mol equiv of dibenzyl disulfide, which proceeds with oxidation of the gallium center and of the dpp-Bian ligand while maintaining coordination of the dpp-Bian ligand (Scheme 1).[20] Just the reverse process, the reduction of dpp-Bian radical anions to dianions takes place in the alkyl radical elimination reactions of the complexes (dpp-Bian)$MgR(Et_2O)$ (R = *i*Pr,[21a] *t*Bu, Me-All[21b]), yielding (dpp-Bian)$Mg(THF)_3$.

Looking for a new generation of redox-active dpp-Bian metal complexes, we turned from the alkaline-earth metals to the lanthanides. The difference between these two groups of elements is the fact that lanthanide compounds in which the metal adopts the valence state 2+ were known only from 7 of the 14 metals, until now. According to the remarkable increase of the reduction potential of divalent lanthanides [$E^0(M^{2+}/M^{3+})$, V] in the order europium (−0.35), ytterbium (−1.15), samarium (−1.55), thulium (−2.3), dysprosium (−2.5), neodymium (−2.6), and lanthanum (−3.1),[22] compounds with divalent europium, samarium, and ytterbium have already been known for more than 90 years,[23] whereas the first molecular species of divalent thulium,[24] dysprosium,[25] and neodymium[25]—the diiodides $LnI_2(L)_n$ (Ln = Tm, Dy, Nd; L = THF, dme)—were prepared by Bochkarev et al. not before the late 1990s. The only known Ln^{II} derivative, [K([2.2.2]crypt)][$LaCp_3$] [Cp = 1,3-bis(trimethylsilyl)cyclopentadiene], was reported by Lappert et al. in 2008.[26] The first scientist who used Ln^{II} compounds, in particular $SmI_2(THF)_n$, as one-electron-reducing agents in organic synthesis was Henri Kagan in 1977.[27] Later on, this

(11) Fedushkin, I. L.; Skatova, A. A.; Ketkov, S. Y.; Eremenko, O. V.; Piskunov, A. V.; Fukin, G. K. *Angew. Chem., Int. Ed.* **2007**, *46*, 4302–4305.
(12) Fedushkin, I. L.; Lukoyanov, A. N.; Ketkov, S. Y.; Hummert, M.; Schumann, H. *Chem.—Eur. J.* **2007**, *13*, 7050–7056.
(13) Fedushkin, I. L.; Lukoyanov, A. N.; Fukin, G. K.; Ketkov, S. Yu.; Hummert, M.; Schumann, H. *Chem.—Eur. J.* **2008**, *14*, 8465–8468.
(14) Hill, N. J.; Vargas-Baca, I.; Cowley, A. H. *Dalton Trans.* **2009**, 240–253.
(15) Schumann, H.; Hummert, M.; Lukoyanov, A. N.; Chudakova, V. A.; Fedushkin, I. L. *Z. Naturforsch.* **2007**, *62b*, 1107–1111.
(16) Fedushkin, I. L.; Maslova, O. V.; Baranov, E. V.; Shavyrin, A. S. *Inorg. Chem.* **2009**, *48*, 2355–2357.
(17) Vasudevan, K.; Cowley, A. H. *Chem. Commun.* **2007**, 3464–3466.
(18) Fedushkin, I. L.; Skatova, A. A.; Lukoyanov, A. N.; Chudakova, V. A.; Dechert, S.; Hummert, M.; Schumann, H. *Russ. Chem. Bull. Int. Ed.* **2004**, *53*, 2751–2762.
(19) Fedushkin, I. L.; Morozov, A. G.; Chudakova, V. A.; Fukin, G. K.; Cherkasov, V. K. *Eur. J. Inorg. Chem.* **2009**, 4995–5003.
(20) Fedushkin, I. L.; Nikipelov, A. S.; Skatova, A. A.; Maslova, O. V.; Lukoyanov, A. N.; Fukin, G. K.; Cherkasov, A. V. *Eur. J. Inorg. Chem.* **2009**, 3742–3749.
(21) (a) Fedushkin, I. L.; Skatova, A. A.; Hummert, M.; Schumann, H. *Eur. J. Inorg. Chem.* **2005**, 1601–1608. (b) Fedushkin, I. L.; Morozov, A. G.; Hummert, M.; Schumann, H. *Eur. J. Inorg. Chem.* **2008**, 1584–1588.
(22) Bünzli, J.-C. G. *Acc. Chem. Res.* **2006**, *39*, 53–61.
(23) Meyer, G. *Chem. Rev.* **1988**, *88*, 93–107.
(24) Bochkarev, M. N.; Fedushkin, I. L.; Fagin, A. A.; Petrovskaya, T. V.; Ziller, J. W.; Broomhall-Dillard, R. N. R.; Evans, W. J. *Angew. Chem., Int. Ed. Engl.* **1997**, *36*, 133–135.
(25) Bochkarev, M. N.; Fagin, A. A. *Chem.—Eur. J.* **1999**, *5*, 2990–2992.
(26) Hitchcock, P. B.; Lappert, M. F.; Maron, L.; Protchenko, A. V. *Angew. Chem., Int. Ed.* **2008**, *47*, 1488–1491.
(27) (a) Namy, J. L.; Girard, P.; Kagan, H. B. *New J. Chem.* **1977**, *1*, 5–7. (b) Girard, P.; Namy, J. L.; Kagan, H. B. *J. Am. Chem. Soc.* **1980**, *102*, 2693–2698. (c) Gopalaiah, K.; Kagan, H. B. *New J. Chem.* **2008**, *32*, 607–637.

Scheme 1. Two-Electron Oxidative Addition of Dibenzyl Disulfide to the Gallium Complex of the dpp-Bian Dianion

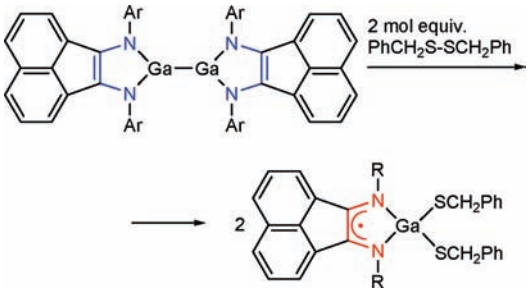

field was further developed especially by Molander,[28] and it still meets great interest of many scientists.[29] Worth mentioning is Evans's decamethylsamarocene, $(C_5Me_5)_2Sm$,[30] which exhibits an amazing reducing power[31] even toward dinitrogen.[32] The diiodides of thulium, dysprosium, and neodymium gave access for the synthesis of their organic derivatives[33] that belong to the strongest reducing agents known so far. In this context, the spontaneous reduction of $[(4\text{-}n\text{Bu-}C_6H_4)_5C_5]_2Sm(CH_2C_6H_4NMe_2\text{-}2)$ to $[(4\text{-}n\text{Bu-}C_6H_4)_5C_5]_2Sm$ caused by benzyl radical elimination[34] is worth mentioning. Because redox reactions of the lanthanides normally are restricted to the transfer of one electron, two-electron-transfer processes, because they are common with transition-metal complexes, thus forming the basis for their catalytic activity, should not be expected of mononuclear lanthanide complexes.[35] However, in this paper we report on the synthesis of (dpp-Bian)Sm(dme)$_3$ (**1**; dme = 1,2-dimethoxyethane), a mononuclear lanthanide complex that, in addition to divalent samarium, contains the dianionic dpp-Bian ligand as a second redox-active center, thus allowing one- as well as two-electron oxidative addition reactions.

Scheme 2. Synthesis of Complex **1**

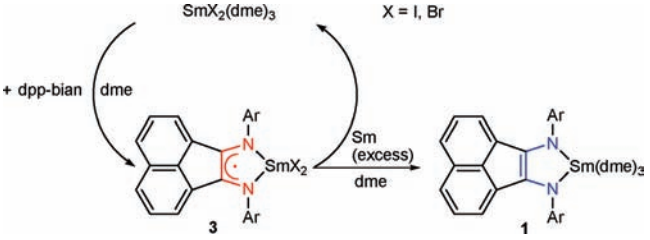

Results and Discussion

Synthesis, Spectroscopic Characterization, and Reactivity of the New Samarium Complexes. The complex **1** has been prepared in analogy to (dpp-Bian)Yb(dme)$_2$[16] by reacting dpp-Bian with an excess of samarium in dme in the presence of catalytic amounts of iodine or 1,2-dibromostilbene; in the absence of halide ions, samarium does not react with dpp-Bian. It is suggested that the first step of the reaction will be the formation of SmI_2 and $SmBr_2$, respectively. The samarium dihalides formed will then reduce dpp-Bian to radical anions, yielding the Sm^{3+} derivatives (dpp-Bian)SmX_2 (X = I, Br), which, in turn, will be reduced by metallic samarium to produce **1** with recovery of the respective samarium dihalide (Scheme 2).

In the course of the reaction, the mixture turns red-brown, and after removal of the solvent, compound **1** remains as a deep-red, almost black, crystalline powder with 85% yield. In contrast to the ytterbium analogue, complex **1** decomposes in a dme solution at room temperature within several hours. Simultaneously, the solution turns blue, the typical color of Sm^{3+} complexes coordinated by dianionic dpp-Bian (vide infra). The limited stability of solutions of **1** prevents the isolation of X-ray quality crystals. However, the paramagnetic complex **1** could be characterized quite sufficiently by its IR and ^{1}H NMR spectra (Figure 1). In its ^{1}H NMR spectrum, the proton signals of the dpp-Bian ligand appear in the expected range (9 to 0 ppm) but are shifted significantly compared to the respective signals of the diamagnetic compound (dpp-Bian)Yb(dme)$_2$.[16] The methyl protons of the four isopropyl groups give rise to

(28) Molander, G. A.; Harris, C. R. *Chem. Rev.* **1996**, *96*, 307–338.
(29) (a) Saadi, J.; Lentz, D.; Reissig, H.-U. *Org. Lett.* **2009**, *11*, 3334–3337. (b) Taaning, R. H.; Lindsay, K. B.; Schioett, B.; Daasbjerg, K.; Skrydstrup, T. *J. Am. Chem. Soc.* **2009**, *131*, 10253–10262. (c) Honda, T.; Hisa, C. *Tetrahedron Lett.* **2009**, *50*, 4654–4657. (d) Yang, B.; Miller, P. A.; Mollmann, U.; Miller, M. J. *Org. Lett.* **2009**, *11*, 2828–2831. (e) Lam, K.; Marko, I. E. *Org. Lett.* **2009**, *11*, 2752–2755. (f) Amiel-Levy, M.; Hoz, S. *J. Am. Chem. Soc.* **2009**, *131*, 8280–8284. (g) Powell, J. R.; Dixon, S.; Light, M. E.; Kilburn, J. D. *Tetrahedron Lett.* **2009**, *50*, 3564–3567. (h) Sun, X.-W.; Xu, M.-H.; Lin, G.-Q. *Tetrahedron Lett.* **2009**, *50*, 3381–3384. (i) Guazzelli, G.; De Grazia, S.; Collins, K. D.; Matsubara, H.; Spain, M.; Procter, D. J. *J. Am. Chem. Soc.* **2009**, *131*, 7214–7215. (j) Masuo, R.; Ohmori, K.; Hintermann, L.; Yoshida, S.; Suzuki, K. *Angew. Chem., Int. Ed.* **2009**, *48*, 3462–3465. (k) Sono, M.; Hanaoaka, M.; Hashimoto, T.; Asakawa, Y.; Tori, M. *Synlett* **2009**, 469–471. (l) Honda, T.; Aranishi, E.; Kaneda, K. *Org. Lett.* **2009**, *11*, 1857–1859. (m) Tsuchida, H.; Tamura, M.; Hasegawa, E. *J. Org. Chem.* **2009**, *74*, 2467–2475. (n) Farran, H.; Hoz, S. *J. Org. Chem.* **2009**, *74*, 2075–2079.
(30) Evans, W. J.; Hughes, L. A.; Hanusa, T. P. *J. Am. Chem. Soc.* **1984**, *106*, 4270–4272.
(31) (a) Evans, W. J.; Grate, J. W.; Hughes, L. A.; Zhang, H.; Atwood, J. L. *J. Am. Chem. Soc.* **1985**, *107*, 3728–3730. (b) Evans, W. J.; Drummond, D. K. *J. Am. Chem. Soc.* **1986**, *108*, 7440–7441. (c) Evans, W. J.; Keyer, R. A.; Zhang, H.; Atwood, J. L. *Chem. Commun.* **1987**, 837–838. (d) Evans, W. J.; Drummond, D. K. *Organometallics* **1988**, *7*, 797–802. (e) Evans, W. J.; Drummond, D. K. *J. Am. Chem. Soc.* **1988**, *110*, 2772–2774. (f) Evans, W. J.; Drummond, D. K.; Chamberlain, L. R.; Doedens, R. J.; Bott, S. G.; Zhang, H.; Atwood, J. L. *J. Am. Chem. Soc.* **1988**, *110*, 4983–4994. (g) Evans, W. J.; Drummond, D. K. *J. Am. Chem. Soc.* **1989**, *111*, 3329–3335. (h) Evans, W. J.; Drummond, D. K. *Organometallics* **1989**, *8*, 573–576. (i) Edelmann, F. T.; Recknagel, A.; Stalke, D.; Roesky, H. W. *Angew. Chem.* **1989**, *101*, 496–497. (j) Evans, W. J.; Keyer, R. A.; Ziller, J. W. *Organometallics* **1990**, *9*, 2628–2631. (k) Recknagel, A.; Noltemeyer, M.; Edelmann, F. T. *J. Organomet. Chem.* **1991**, *410*, 53–61. (l) Evans, W. J.; Keyer, R. A.; Ziller, J. W. *Organometallics* **1993**, *12*, 2618–2633. (m) Evans, W. J.; Gonzales, S. L.; Ziller, J. W. *J. Am. Chem. Soc.* **1994**, *116*, 2600–2608. (n) Hou, Z.; Fujita, A.; Zhang, Y.; Miyano, T.; Yamazaki, H.; Wakatsuki, Y. *J. Am. Chem. Soc.* **1998**, *120*, 754–766. (o) Evans, W. J.; Seibel, C. A.; Ziller, J. W. *Inorg. Chem.* **1998**, *37*, 770–776. (p) Hou, Z.; Yoda, C.; Koizumi, T.; Nishiura, M.; Wakatsuki, Y.; Fukuzawa, S.; Takats, J. *Organometallics* **2003**, *22*, 3586–3592. (q) Evans, W. J.; Montalvo, E.; Foster, S. E.; Harada, K. A.; Ziller, J. W. *Organometallics* **2007**, *26*, 2904–2910.
(32) Evans, W. J.; Ulibarri, T. A.; Ziller, J. W. *J. Am. Chem. Soc.* **1988**, *110*, 6877–6879.
(33) (a) Evans, W. J.; Allen, N. T.; Ziller, J. W. *J. Am. Chem. Soc.* **2001**, *123*, 7927–7928. (b) Evans, W. J.; Allen, N. T.; Ziller, J. W. *Angew. Chem., Int. Ed.* **2002**, *41*, 359–361. (c) Nief, F.; Turcitu, D.; Ricard, L. *Chem. Commun.* **2002**, 1646–1647. (d) Evans, W. J.; Zucchi, G.; Ziller, J. W. *J. Am. Chem. Soc.* **2003**, *125*, 10–11. (e) Turcitu, D.; Nief, F.; Ricard, L. *Chem.—Eur. J.* **2003**, *9*, 4916–4923. (f) Nief, F.; De Borms, B. T.; Ricard, L.; Carmichael, D. *Eur. J. Inorg. Chem.* **2005**, 637–643. (g) Jaroschik, F.; Nief, F.; Ricard, L. *Chem. Commun.* **2006**, 426–428. (h) Jaroschik, F.; Nief, F.; Le Goff, X.-F.; Ricard, L. *Organometallics* **2007**, *26*, 1123–1125. (i) Jaroschik, F.; Nief, F.; Le Goff, X.-F.; Ricard, L. *Organometallics* **2007**, *26*, 3552–3558. (j) Jaroschik, F.; Momin, A.; Nief, F.; Le Goff, X.-F.; Deacon, G. B.; Junk, P. C. *Angew. Chem., Int. Ed.* **2009**, *48*, 1117–1121.
(34) Ruspic, C.; Moss, J. R.; Schuermann, M.; Harder, S. *Angew. Chem., Int. Ed.* **2008**, *47*, 2121–2126.
(35) Ewans, W. J. *Inorg. Chem.* **2007**, *46*, 3435–3449.

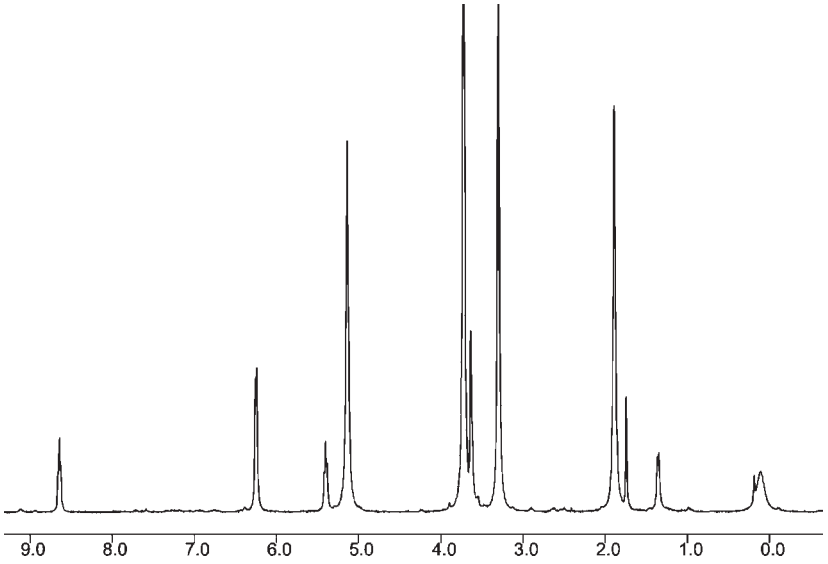

Figure 1. ^{1}H NMR spectrum of complex **1** (THF-d_8, 293 K, 200 MHz).

two singlets at δ = 5.14 and 1.89 ppm and the appropriate methine protons to one singlet at δ = 0.11 ppm. The signals of the six pairs of aromatic protons appear at δ = 8.64 (2 H), 6.25 (4 H), 5.40 (2 H), 3.63 (2 H), and 1.35 (2 H) ppm. The shifts of the two singlet signals of the dme protons (δ = 3.72 and 3.30 ppm) correspond with those of free dme, thus indicating replacement of the dme ligands in **1** by THF-d_8. The oxidation state of the samarium metal in complex **1** is deduced from the measurement of the magnetic susceptibility of complex **1** in a THF solution by the Evans method. The determined magnetic moment of **1** at 298 K is 3.61 μ_B, a value that corresponds perfectly to that observed in the Sm^{II} complexes.[22]

The IR spectrum of **1** also confirms the dianionic character of the dpp-Bian ligand. While the spectrum of free dpp-Bian shows three C=N stretching vibrations at 1671, 1652, and 1642 cm^{-1} as the strongest absorptions,[36] the spectrum of **1** shows only one C−N stretching vibration at 1304 cm^{-1} as the most intense absorption associated with the dpp-Bian ligand.

Because of the presence of two redox-active centers in **1**, a one-electron oxidation may occur either by oxidation of the dianionic dpp-Bian ligand to a radical anion or by oxidation of Sm^{II} to Sm^{III}. In contrast to the reaction of the Yb^{II} complex (dpp-Bian)Yb(dme)$_2$ with 0.5 mol equiv of Ph(Br)CHCH(Br)Ph, which causes oxidation of the dianionic ligand to the dpp-Bian radical anion and formation of the Yb^{II} complex [(dpp-Bian)YbBr(dme)]$_2$ (Chart 1B),[16] the analogous reaction of complex **1** proceeds with oxidation of the metal center and formation of the Sm^{III} complex [(dpp-Bian)SmBr(dme)]$_2$ (**2**; Scheme 3). According to the transition $Sm^{II} \rightarrow Sm^{III}$, the reaction is accompanied with a color change of the dme solution from red-brown to deep blue. Complex **2** was isolated from benzene as deep-blue crystals with 43% yield. The UV−vis spectrum of **2** in THF exhibits absorption at 640 nm. For comparison, the related Nd^{III} complex [(dpp-Bian)NdCl(THF)$_2$]$_2$[15] reveals an absorption at 671 nm. In contrast to the Sm^{II} derivative **1**, the ^{1}H NMR spectrum of the paramagnetic Sm^{III} complex **2** does not reveal any significant perturbation in the NMR chemical shifts (Figure 2).

The 12 aromatic protons of the dpp-Bian ligand are equivalent in pairs and result in five broadened signals in the range δ = 7.79−7.02 ppm [7.79 (2 H), 7.63 (4 H), 7.29 (2 H), 7.20 (2 H), and 7.02 (2 H)]. The integral intensity of the benzene proton signal (δ = 7.38 ppm, 9 H) corresponds exactly to one and a half benzene molecules (per one monomeric unit) present in the crystal lattice of complex **2**. Also, the intensities of the signals of dme molecules [δ = 3.46 (4 H) and 3.32 (6 H) ppm] indicate the presence of one dme ligand per one samarium atom. Nonequivalent methyl groups of the isopropyl substituents give rise to two broadened signals at δ = 1.89 (12 H) and 1.23 (12 H) ppm. Unexpectedly, the signal of the methine protons could not be observed in the spectrum, probably because of broadening of the signal. The magnetic moment of complex **2** (1.76 μ_B per samarium ion, 298 K, THF) is somewhat higher than expected for Sm^{III} species (1.55 μ_B).[22] It is worth pointing out that the crystal and molecular structures of **2** and **B** are very much alike, although their electronic structures are very different (the crystal data for **2** are given in Table 1 [crystal data for **B**·2dme: $P\bar{1}$, a = 11.7726(9) Å, b = 14.0198(11) Å, c = 14.8144(12) Å, α = 63.7110(10)°, β = 84.042(2)°, γ = 75.145(2)°].

Oxidation of both redox-active centers of **1** takes place if it is reacted with equimolar amounts of 1,2-dibromostilbene, yielding (dpp-Bian)$SmBr_2$(dme)$_2$ (**3**; Scheme 3), accompanied by a change of the color of the reaction mixture from red-brown to cherry red, thus indicating the formation of dpp-Bian radical anions. The reaction product **3** was isolated from toluene as deep-red crystals in 40% yield.

In the coordination chemistry of the transition metals, there are several documented mechanisms for oxidative additions. They include (i) concerted, associative,

(36) (a) Paulovicova, A. A.; El-Ayaan, U.; Shibayama, K.; Morita, T.; Fukuda, Y. *Eur. J. Inorg. Chem.* **2001**, 2641–2646. (b) Paulovicova, A. A.; El-Ayaan, U.; Umezava, K.; Vithana, C.; Ohashi, Y.; Fukuda, Y. *Inorg. Chim. Acta* **2002**, *339*, 209–214.

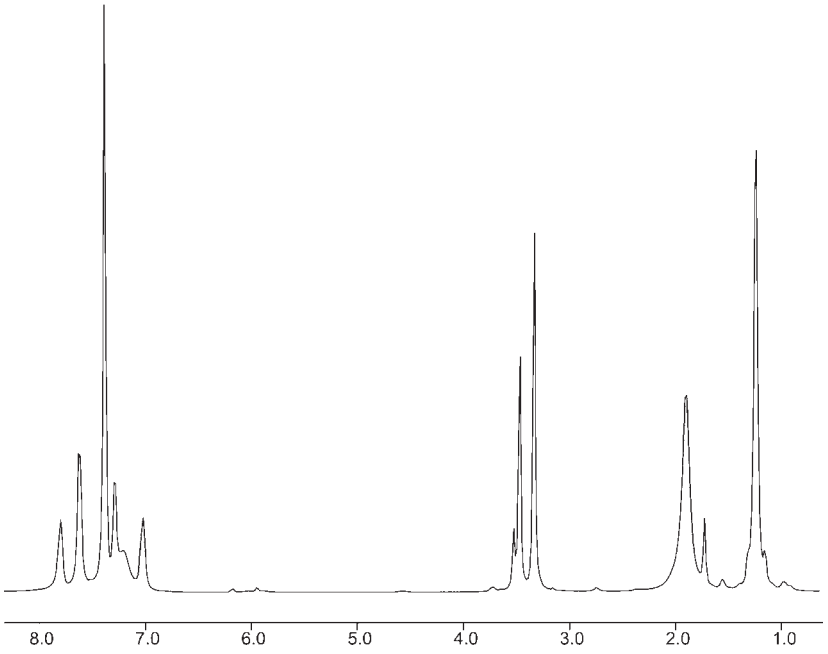

Figure 2. ^{1}H NMR spectrum of complex **2** (THF-d_8, 293 K, 400 MHz).

Scheme 3. Formation of Complexes **2** and **3**

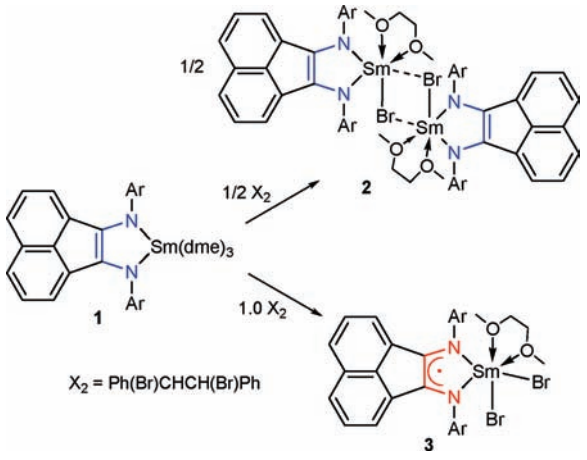

one-step insertions, (ii) ionic, associative, two-step S_N2 reactions, and (iii) electron-transfer/radical-chain mechanisms.[37] The process of the formation of complex **3** differs for all three mechanisms, although it has some similarity to the third one, which is best represented by the addition of alkyl halides RX to the Vaska complex $L_2Ir(CO)Cl$ ($L = PPh_3$). In the case of the Vaska complex, the reaction starts with the reduction of the radical $R^\bullet$ (generated from RX under irradiation or in the presence of dioxygen) by Ir^I to give the Ir^{II} intermediate $L_2IrR(CO)Cl$, which, in turn, reacts with RX, forming the Ir^{III} complex $L_2IrR(CO)(Cl)X$[38] as the final product of a two-electron oxidative addition along with the radical $R^\bullet$ that propagates the reaction chain. As in the case of the Vaska complex, the oxidation of **1** with 1 mol equiv of bromine proceeds stepwise with a transfer of one and then another electron to a substrate.

The complex (dpp-Bian)$SmI_2(THF)_2$ (**4**), the analogue to the bromine derivative **3**, can be prepared by two-electron oxidation of **1** with equimolar amounts of iodine. Similar processes—halide-based oxidation of the coordinated dianonic ligand—have been observed by Heyduk and co-workers on the zirconium complexes with two amidophenolate redox-active ligands.[39] Alternatively, complex **4** can be prepared by the reaction of dpp-Bian with an equimolar amount of samarium diiodide (Scheme 4). Both reactions proceed instantly upon mixing of the reagents at ambient temperature in THF and afford cherry-red solutions of **4**. The complex was isolated as deep-red prismatic crystals from diethyl ether with yields of 65−82%.

The fact that (dpp-Bian)SmI[SC(S)NMe_2](dme) (**5**) can be prepared by the successive addition of 0.5 mol equiv of iodine and 0.5 mol equiv of tetramethylthiuram disulfide to solutions of **1** (Scheme 5) proves the in situ generation of [(dpp-Bian)SmI(dme)]$_2$ and, hence, the ability of **1** to react with iodine also by one-electron oxidation. Compound **5** was isolated as deep-red, prismatic crystals with 69% yield. [(dpp-Bian)SmI(O*t*Bu)(THF)]$_2$ (**6**), also a deep-red, crystalline Sm^{III} complex supported by radical-anionic dpp-Bian, has been obtained with 73% yield by metathesis of (dpp-Bian)$SmI_2(THF)_2$ (**4**) with *t*BuOK (Scheme 6).

Main-group metal complexes containing the dpp-Bian radical anion can be easily characterized by electron spin resonance (ESR) spectroscopy because the radical ligand reveals a well-resolved quintet arising from the coupling of the unpaired electron with the two nitrogen nuclei. Because of the presence of paramagnetic samarium ions and dpp-Bian radical anions in complexes **3**−**6**, their

(37) Hegedus, L. *Transition Metals in the Synthesis of Complex Organic Molecules*; University Science Books: Sausalito, CA, 1999; p 20.

(38) (a) Labinger, J. R.; Osborn, J. A. *Inorg. Chem.* **1980**, *19*, 3230–3235. (b) Labinger, J. R.; Osborn, J. A.; Coville, N. J. *Inorg. Chem.* **1980**, *19*, 3236–3243. (c) Jenson, F. R.; Knickel, B. *J. Am. Chem. Soc.* **1971**, *93*, 6339–6340.

(39) Blackmore, K. J.; Ziller, J. W.; Heyduk, A. F. *Inorg. Chem.* **2005**, *44*, 5559–5561.

Table 1. Crystal Data and Structure Refinement Details for Compounds **2**−**6**

	2	**3**	**4**	**5**	**6**
formula	$C_{80}H_{100}Br_2N_4O_4Sm_2 \cdot 3C_6H_6$	$C_{40}H_{50}Br_2N_2O_2Sm \cdot {}^1/_2C_7H_8$	$C_{44}H_{56}I_2N_2O_2Sm$	$C_{43}H_{56}IN_3O_2S_2Sm \cdot C_4H_{10}O_2$	$C_{88}H_{114}I_2N_4O_4Sm_2 \cdot C_6H_{14}$
M_r [g mol^{-1}]	1876.48	947.06	1049.06	1078.40	1932.50
cryst syst	triclinic	monoclinic	orthorhombic	monoclinic	monoclinic
space group	$P\bar{1}$	$P2_1/c$	$P2_12_12_1$	$C2/c$	$P2_1/n$
a [Å]	11.854(5)	19.9920(11)	11.516(5)	35.918(5)	16.136(5)
b [Å]	14.296(5)	14.1640(7)	17.618(5)	16.717(5)	16.036(5)
c [Å]	14.505(5)	15.426(1)	21.407(5)	28.031(5)	18.866(5)
α [deg]	64.940(5)	90	90	90	90
β [deg]	83.343(5)	106.641(6)	90	139.806(5)	109.302(5)
γ [deg]	86.159(5)	90	90	90	90
V [Å^3]	2211.0(1)	4185.2(4)	4343.0(2)	10862(4)	4607(2)
Z	1	4	4	8	2
ρ_{calc} [g cm^{-3}]	1.409	1.503	1.604	1.319	1.393
μ [mm^{-1}]	2.271	3.349	2.809	1.765	1.981
$F(000)$	960	1908	2072	4384	1964
crystal size, [mm^3]	0.11 × 0.09 × 0.05	0.21 × 0.11 × 0.01	0.12 × 0.11 × 0.10	0.25 × 0.23 × 0.13	0.24 × 0.17 × 0.14
$\theta_{min}/\theta_{max}$ [deg]	3.09/30.00	3.02/25.00	2.99/27.00	3.00/30.00	2.96/27.50
index ranges	$-16 \le h \le 16$	$-23 \le h \le 22$	$-14 \le h \le 14$	$-50 \le h \le 50$	$-20 \le h \le 20$
	$-18 \le k \le 20$	$-16 \le k \le 10$	$-22 \le k \le 22$	$-21 \le k \le 23$	$-19 \le k \le 20$
	$-19 \le l \le 20$	$-15 \le l \le 18$	$-27 \le l \le 27$	$-39 \le l \le 39$	$-22 \le l \le 23$
reflns collected	30 060	20 306	53 270	59 890	27 964
indep reflns	12 858	7349	9474	15 786	10 269
R_{int}	0.0462	0.1175	0.0739	0.0388	0.0373
max/min transmn	0.8949/0.7883	0.9673/0.5398	0.7664/0.7292	0.8030/0.6667	0.7689/0.6478
data/restraints/param	12 858/0/506	7349/0/434	9474/30/464	15 786/0/481	10 269/0/463
GOF on F^2	0.898	0.853	1.185	0.983	0.891
final R indices [$I > 2\sigma(I)$]	R1 = 0.0349	R1 = 0.0613	R1 = 0.0777	R1 = 0.0413	R1 = 0.0301
	wR2 = 0.0498	wR2 = 0.1292	wR2 = 0.1473	wR2 = 0.0964	wR2 = 0.0574
R indices (all data)	R1 = 0.0658	R1 = 0.1590	R1 = 0.1043	R1 = 0.0695	R1 = 0.0555
	wR2 = 0.0553	wR2 = 0.1454	wR2 = 0.1562	wR2 = 0.1030	wR2 = 0.0604
largest diff peak/hole [e Å^{-3}]	0.937/−0.813	1.118/−1.241	2.004/−1.659	1.514/−0.890	1.204/−0.564

Scheme 4. Two Synthetic Pathways for the Preparation of **4**

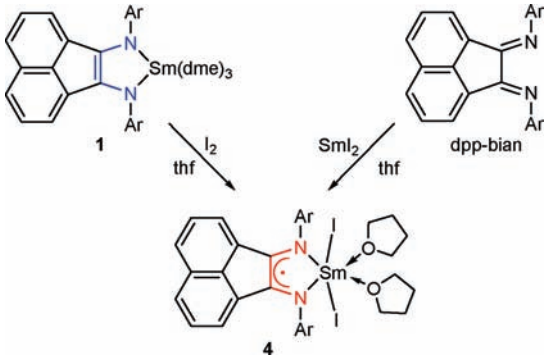

Scheme 5. Synthesis of **5**

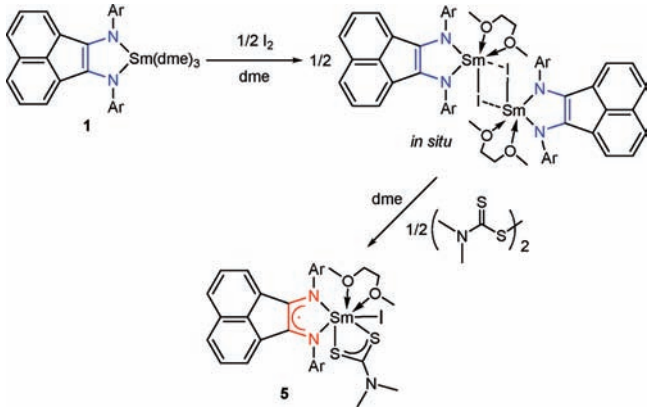

Scheme 6. Synthesis of **6**

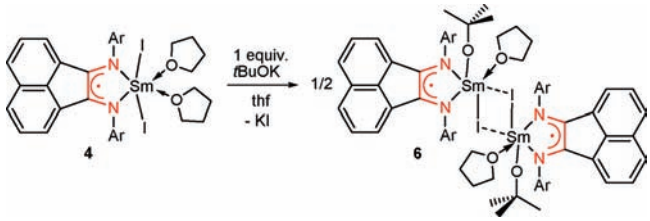

characterization by ESR and ^{1}H NMR spectroscopy is excluded. The magnetic moment of complex **6** (2.16 μ_B per samarium ion, 298 K, THF) is somewhat lower than that calculated for a system with one paramagnetic Sm^{III} center and one radical anion of dpp-Bian [$\mu = (1.55^2 + 1.73^2)^{1/2} = 2.32\ \mu_B$]. Single-crystal X-ray diffraction analyses of **3** and **6** have proven their constitution.

Molecular Structures. The molecular structures of complexes **2**−**6** were determined by single-crystal X-ray diffraction and are depicted in Figures 3−7. The crystal data collections and structure refinement details are listed in Table 1 and selected bond lengths and bond angles in Tables 2 and 3.

2 is a centrosymmetric dimer formed from the monomers by bridging bromine atoms. The dimer shows an inversion center located in the middle of the two samarium atoms, which are coordinated in a distorted octahedral fashion. The samarium atoms deviate 0.573 Å from the respective N(1)−C(1)−C(2)−N(2) plane. As in the related ytterbium complex (dpp-Bian)Yb(dme)$_2$ (**B**)[16] (cf. Table 2), the metal−nitrogen distances in **2** are very close [2.263(2) and 2.259(2) Å], while the metal−oxygen(dme) and the metal−bromine distances are quite different among one another [Sm(1)−O(1) 2.519(1) Å and

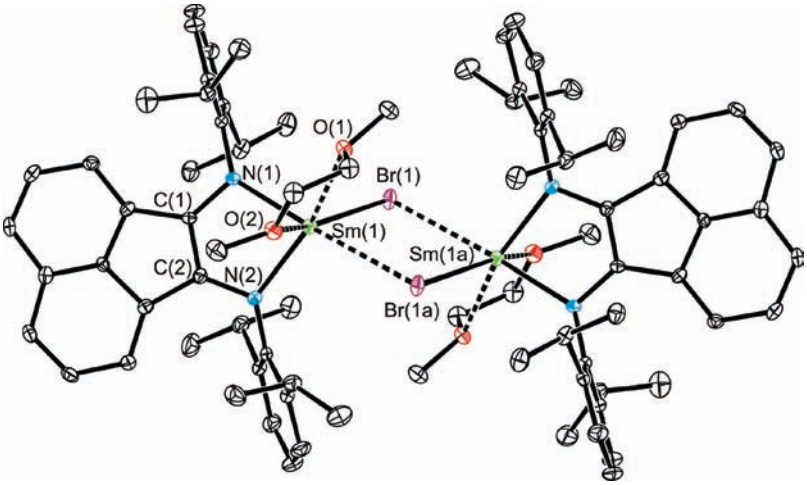

Figure 3. Molecular structure of **2**. Thermal ellipsoids are drawn at the 30% probability level. Hydrogen atoms are omitted.

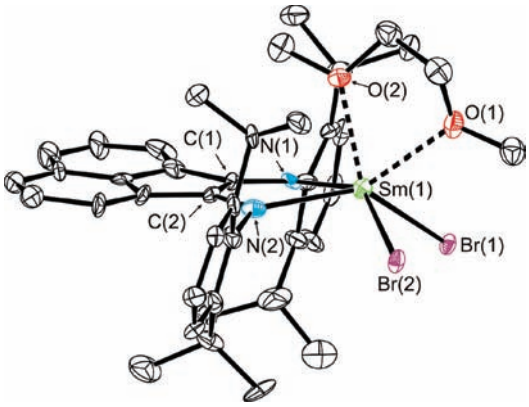

Figure 4. Molecular structure of **3**. Thermal ellipsoids are drawn at the 30% probability level. Hydrogen atoms are omitted.

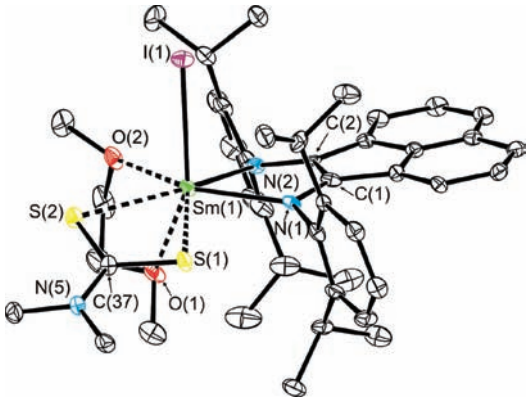

Figure 6. Molecular structure of **5**. Thermal ellipsoids are drawn at the 30% probability level. Hydrogen atoms are omitted for clarity.

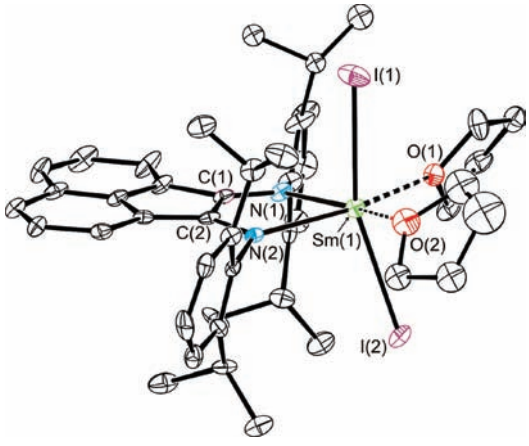

Figure 5. Molecular structure of **4**. Thermal ellipsoids are drawn at the 20% probability level. Hydrogen atoms are omitted.

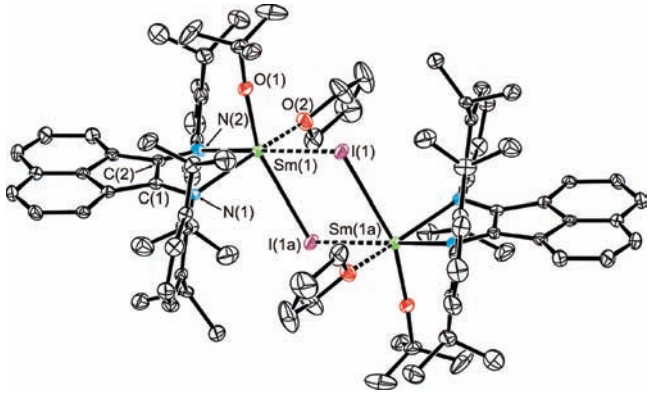

Figure 7. Molecular structure of **6**. Thermal ellipsoids are drawn at the 30% probability level. Hydrogen atoms are omitted.

Sm(1)−O(2) 2.444(1) Å; Sm(1)−Br(1) 2.9148(8) Å and Sm(1)−Br(1a) 3.0532(8) Å]. These differences explain the trans effect of the nitrogen atoms N(2) and N(1), which are trans-positioned to O(1) and Br(1a), respectively. So far, the structures of only three samarium complexes containing the cyclic (Sm-μ-Br)$_2$ unit have been reported and can be used for comparison. Thus, the Sm−Br distances in [(quaph)(THF)$_2$Sm(μ-Br)]$_2$ (quaph = *o*-tetraphenylene)[40a] and [Br(dme)$_2$Sm(μ-Br)]$_2$[40b] differ only slightly (2.986/2.992 and 3.080/3.083 Å, respectively) and are of equal length in [{(Me$_3$Si)$_2$N}$_2$Sm(μ-Br)(THF)]$_2$ (2.955 Å).[40c] The fact that the Sm−N distances in **2** are 0.17 Å shorter than the Yb−N distances in **B** (Table 2) in which Yb^{2+} ions are coordinated to radical-anionic

(40) (a) Boje, B.; Magull, J. *Z. Anorg. Allg. Chem.* **1994**, *620*, 703–706. (b) Mandel, A.; Magull, J. *Z. Anorg. Allg. Chem.* **1997**, *623*, 1542–1546. (c) Karl, M.; Seybert, G.; Massa, W.; Agarwal, S.; Greiner, A.; Dehnicke, K. *Z. Anorg. Allg. Chem.* **1999**, *625*, 1405–1407.

Table 2. Selected Bond Lengths [Å] and Angles [deg] in **B** and **2**−**4**

	B[a]	**2**[b]	**3**[b]	**4**[c]
M(1)−N(1)	2.427(4)	2.263(2)	2.428(9)	2.430(8)
M(1)−N(2)	2.430(4)	2.259(2)	2.462(9)	2.428(8)
M(1)−O(1)	2.478(3)	2.519(1)	2.458(8)	2.434(7)
M(1)−O(2)	2.423(4)	2.444(1)	2.447(8)	2.43(2)
M(1)−Hal(1)	2.867(1)	2.9148(8)	2.860(1)	3.056(1)
M(1)−Hal(1a)	2.932(1)	3.0532(8)		
M(1)−Hal(2)			2.836(1)	3.031(1)
N(1)−C(1)	1.338(6)	1.403(3)	1.30(1)	1.33(1)
N(2)−C(2)	1.354(6)	1.397(3)	1.33(1)	1.33(1)
C(1)−C(2)	1.452(7)	1.384(3)	1.44(1)	1.44(1)
Hal(1)−M(1)−Hal(1a)	84.41(1)	78.42(3)		
Hal(1)−M(1)−Hal(2)			97.15(4)	160.62(4)
O(1)−M(1)−O(2)	64.4(1)	64.58(6)	65.3(3)	111.0(6)
N(1)−M(1)−N(2)	71.6(1)	78.20(7)	69.0(3)	70.8(3)

[a] M = Yb, Hal = Br. [b] M = Sm, Hal = Br. [c] M = Sm, Hal = I.

Table 3. Selected Bond Lengths [Å] and Angles [deg] in **5** and **6**

	5	**6**
Sm(1)−N(1)	2.463(3)	2.460(3)
Sm(1)−N(2)	2.485(3)	2.447(3)
Sm(1)−O(1)	2.535(3)	2.049(2)
Sm(1)−O(2)	2.541(2)	2.442(2)
Sm(1)−S(1)	2.812(1)	
Sm(1)−S(2)	2.856(1)	
Sm(1)−I(1)	3.0614(6)	3.2269(7)
Sm(1)−I(2)		
Sm(1)−I(1a)		3.2302(8)
N(1)−C(1)	1.332(4)	1.336(4)
N(2)−C(2)	1.329(4)	1.330(4)
C(1)−C(2)	1.445(4)	1.447(4)
I(1)−Sm(1)−I(2)		78.10(1)
N(1)−Sm(1)−O(1)	87.52(6)	101.64(9)
N(1)−Sm(1)−O(2)	152.41(5)	150.97(8)
N(2)−Sm(1)−O(1)	86.40(9)	98.25(8)
N(2)−Sm(1)−O(2)	82.06(8)	83.83(9)
N(2)−Sm(1)−S(2)	155.60(6)	
O(1)−Sm(1)−O(2)	65.32(8)	94.97(9)
N(1)−Sm(1)−N(2)	68.79(8)	70.43(9)
S(1)−Sm(1)−S(2)	62.87(3)	
O(1)−Sm(1)−I(1)		83.44(6)

dpp-Bian ligands reflects the different oxidation state of samarium in **2**. On the basis of the values of the radii of the seven-coordinate ions Sm^{3+}, Sm^{2+}, Yb^{3+}, and Yb^{2+} (1.02, 1.22, 0.93, and 1.08 Å, respectively[41]), the shorter Sm−N distances clearly indicate the oxidation state Sm^{3+} because otherwise the Sm−N distances in **2** should be longer than the Yb−N distances in **B**. As a consequence, the dpp-Bian ligand in **2** has to adopt a dianionic state, which can definitely be proven by inspection of the bond distances within the diimine moiety because each reduction state of the dpp-Bian ligand—neutral, radical-anionic, or dianionic—has its own structural fingerprint. The increasing population of the lowest unoccupied molecular orbital of dpp-Bian on going from its neutral to its radical-anionic state and further to its dianionic state results in a progressive shortening of the C(1)−C(2) bond and, simultaneously, in a progressive elongation of the C(1)−N(1) and C(2)−N(2) bonds. The distances C(1)−N(1) and C(2)−N(2) of the dpp-Bian ligand in **2** [1.403(3) and 1.397(3) Å] are longer than those in free dpp-Bian [both 1.282(4) Å][42] and longer than those in **B** [1.338(6) and 1.354(6) Å] containing radical-anionic dpp-Bian ligands but close to those of the dianionic dpp-Bian ligand in $(dpp\text{-}Bian)Mg(THF)_3$[9a] [1.401(6) and 1.378(7) Å]. All of these structural facts confirm that complex **2** consists of dpp-Bian dianions coordinated to Sm^{3+} ions.

Compounds **3** and **4** represent monomeric samarium species with a distorted octahedral ligand arrangement around the metal atoms. Because of the chelating character of the dme ligand [the bite angle O(1)−M(1)−O(2) is 65.3(3)°], the bromine atoms in **3** are cis-configured between each other [Br(1)−Sm(1)−Br(2) 97.15(4)°], whereas the iodine atoms in **4** occupy the axial positions of the distorted octahedron [I(1)−Sm(1)−I(2) 160.62(4)°]. The deviation of the samarium atom from the respective N(1)−C(1)−C(2)−N(2) plane of the dpp-Bian ligand is 0.396 Å in **3** and 0.406 Å in **4**. As expected, the distances of the samarium atom to the terminal bromine atoms in **3** [Sm(1)−Br(1) 2.860(1) Å and Sm(1)−Br(2) 2.836(1) Å] are notably shorter than those to the bridging bromine atoms in **2**. The difference between the Sm−I distances in **4** [Sm(1)−I(1) 3.056(1) Å and Sm(1)−I(2) 3.031(1) Å] is of the same order as the difference between the Sm−Br distances in **3**. The Sm−N bonds in **3** and **4** [**3**, 2.428(9) and 2.462(9) Å; **4**, 2.430(8) and 2.428(8) Å] are significantly longer compared to the Sm−N bonds in complex **2** [2.263(2) and 2.259(2) Å], thus indicating a weaker interaction of the Sm^{3+} ion with the dpp-Bian radical anion in **3** and **4** than with the dpp-Bian dianion in **2**. Again, the radical-anionic nature of the dpp-Bian ligand in **3** and **4** can be deduced from the bond lengths of the C−N and C−C bonds of the coordinating part of the ligand. Thus, the C(1)−N(1) and C(2)−N(2) bonds in **3** [1.30(1) and 1.33(1) Å, respectively] and **4** [both 1.33(1) Å] are longer than the corresponding bonds in free dpp-Bian (vide supra) but shorter than those in the dpp-Bian dianion of **2** (Table 2).

The molecules of complex **5** show a seven-coordinated samarium ion in an irregular coordination sphere. Obviously, because of the higher coordination number of the metal, the Sm(1)−I(1) bond [3.0614(6) Å] is somewhat longer than those in **4**, the Sm−N distances [Sm(1)−N(1) 2.463(3) Å and Sm(1)−N(2) 2.485(3) Å] are longer compared to those in **3** [2.428(9) and 2.462(9) Å] and **4** [2.430(8) and 2.428(8) Å], and the distances between the samarium atom and the coordinated neutral dme molecules increase by 0.08 Å on going from **3** to **5** (Tables 2 and 3). As in **2**, the strong nucleophilicity of the nitrogen atoms of the dpp-Bian ligand causes an elongation of the bonds of Sm(1) to O(2) and S(2); those atoms are trans-positioned to N(1) and N(2) [Sm(1)−O(2) 2.541(2) Å > Sm(1)−O(1) 2.535(3) Å; Sm(1)−S(2) 2.856(1) Å > Sm(1)−S(1) 2.812(1) Å]. A closer look at these distances reveals that the greater difference in the lengths of the two Sm−S bonds compared to the difference of the two Sm−O bonds corresponds to the shorter Sm−N(2) bond compared to the Sm−N(1) bond. Thus, the dpp-Bian ligand in **5** may be best represented by the resonance structure depicted in Figure 8. The alterations of the C−N and C−C bond lengths within the metallacycle in **5**

(41) Shannon, R. D. *Acta Crystallogr., Sect. A* **1976**, *32*, 751–767.

(42) Fedushkin, I. L.; Chudakova, V. A.; Fukin, G. K.; Dechert, S.; Hummert, M.; Schumann, H. *Russ. Chem. Bull.* **2004**, *53*, 2744–2750.

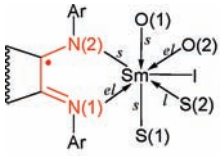

Figure 8. Dominating resonance structure of the dpp-Bian radical anion in complex **5** that determines alteration of the Sm−S and Sm−O bond distances. The naphthalene part of the dpp-Bian ligand and the bonds within dme and the dithiocarbamate fragments are omitted for clarity.

indicate the radical-anionic character of the dpp-Bian ligand.

Complex **6**, a centrosymmetric dimer formed from the monomers by bridging iodine atoms, shows an inversion center located in the middle between the two six-coordinated samarium atoms. Up to now, only three samarium complexes have been investigated by X-ray crystallography in which iodine and alkoxy or aryloxy ligands are present at the same time, which are the monomeric Sm^{III} derivatives $(t\text{BuO})SmI_2(THF)_4$[43a] and (4-Me-2,6-$tBu_2$-$C_6H_2O)_2SmI(THF)_2$[43b] and the dimeric, iodine-bridged Sm^{II} complex $[(4\text{-Me-2,6-}t\text{Bu}_2C_6H_2O)_2SmI(THF)_2]_2$.[43b] The reason for the formation of samarium−iodine bridges instead of samarium−alkoxide bridges probably will be the resulting larger space between the metals and the bulky dpp-Bian ligands.

The fact that, in contrast to complex **2**, the samarium−iodine bonds in **6** are almost of equal length [Sm(1)−I(1) 3.2269(7) Å and Sm(1)−I(1a) 3.2302(8) Å] seems very strange at first glance. It may be explained that, in contrast to **2**, each halide atom of **6** is not only influenced by the nucleophilic N(2) atom of the dpp-Bian ligand but also by the nucleophilic O(1) atom of the alkoxide group. As in complexes **3**−**5**, the C−N and C−C bond lengths within the metallacycle indicate the radical-anionic character of the dpp-Bian ligand in **6**. The Sm−N bond lengths in **6** [Sm(1)−N(1) 2.460(3) Å and Sm(1)−N-(2) 2.447(3) Å] are in the range of the analogous distances in **4** and **5**.

Conclusion

The samarium complex **1** can be synthesized by oxidation of metallic samarium with dpp-Bian in the presence of catalytic amounts of iodine. Because complex **1** consists of the redox-active Sm^{II} ion and the redox-active dpp-Bian dianion, it is capable undergoing two-electron oxidative addition reactions. In fact, such reactions include two successive one-electron-transfer reactions. In the case of **1**, the metal is getting oxidized initially, while in the case of the ytterbium analogue (dpp-Bian)Yb(dme)$_2$, oxidation of the dpp-Bian ligand takes place first.[16] This is in accordance with the reduction potential of the dpp-Bian radical anion (−1.0 V),[44] which is closer to the reduction potential of Yb^{II} (−1.15 V) than to that of Sm^{II} (−1.55 V).[22] To generate Bian−lanthanide complexes, which may compete with the transition-metal-based catalytic systems, they should be able to undergo two-electron reductive elimination. Possibilities of getting closer to this goal are to influence the reduction potential of the Bian ligands by introduction of π-electron-donating groups into their naphthalene core and/or by a careful choice of the lanthanide metals. The study of the molecular structures of the dpp-Bian samarium complexes **2**−**6** has revealed that the coordination strength of the spectator ligands, i.e., anionic ligands like halide ions and dithiocarbamates, or coordinating solvents, may be affected by the rigid chelating anionic dpp-Bian ligand. Also, a temperature-induced interconversion between the redox isomers $(\text{diimine})^{-1}Sm^{2+}X$ and $(\text{diimine})^{-2}Sm^{3+}X$ (X = spectator ligand) might be expected provided that the right redox-active diimine has been selected.

Experimental Section

General Remarks. All manipulations were carried out in a vacuum or under nitrogen by using Schlenk techniques. The solvents 1,2-dimethoxyethane (dme), tetrahydrofuran (THF), toluene, benzene, and hexane were distilled from sodium benzophenone prior to use. 1,2-Bis[(2,6-diisopropylphenyl)imino]-acenaphthene (dpp-Bian) was prepared by condensation of acenaphthenequinone with 2,6-diisopropylaniline (both from Aldrich) in refluxing acetonitrile. The reactants $[(CH_3)_2NC(S)S]_2$ and tBuOK were purchased from Aldrich and used without further purification. THF-d_8, used for ^{1}H NMR measurement, was dried over sodium benzophenone at ambient temperature and was, just prior to use, condensed under a vacuum into the NMR tube already containing compound **1** or **2**. The melting points were measured in sealed capillaries. The IR spectra were recorded on a FSM-1201 and Vertex 70 spectrometer, the ^{1}H NMR spectra on Bruker DPX 200 and Bruker Avance III instruments, and the UV−vis spectrum on a Perkin-Elmer λ 25 spectrometer.

(dpp-Bian)Sm(dme)$_3$ (1). The mixture of samarium metal (5.5 g, 36.6 mmol) and I_2 (13 mg, 0.05 mmol) in dme (30 mL) was stirred at ambient temperature until the color of the solution turned blue. Then dpp-Bian (0.5 g, 1.0 mmol) was added to the reaction mixture, which turned red-brown within 30 min of reflux. Slow evaporation of the solvent from the decanted solution afforded compound **1** (0.78 g, 85%) as a deep-red crystalline powder. Mp: 265 °C (dec). ^{1}H NMR (THF-d_8, 200 MHz): δ 8.64 (dd, J = 7.5 and 6.2 Hz, 2 H, CH arom.), 6.25 (d, J = 7.5 Hz, 4 H, CH arom.), 5.40 (dd, J = 6.2 and 7.5 Hz, 2 H, CH arom.), 5.14 (s, 12 H, CH(CH_3)$_2$), 3.72 (s, 18 H, CH_3(dme)), 3.63 (s, 2 H, CH arom.), 3.30 (s, 12 H, CH_2(dme)), 1.89 (s, 12 H, CH(CH_3)$_2$), 1.35 (d, J = 5.0, 2 H, CH arom.), 0.11 (s, 4 H, CH(CH$_3$)$_2$). IR (Nujol): ν 1669 w, 1642 w, 1606 w, 1585 m, 1574 m, 1415 s, 1365 w, 1349 w, 1304 s, 1247 s, 1210 m, 1191 m, 1172 s, 1107 s, 1061 s, 1026 w, 997 w, 977 w, 935 w, 918 s, 882 w, 853 s, 807 m, 791 m, 762 s, 751 s, 740 w, 708 w, 690 w, 680 s, 616 m, 596 w, 536 w, 512 w, 488 w cm^{-1}. Anal. Calcd for $C_{48}H_{70}N_2O_6Sm$ (921.45): C, 62.57; H, 7.66. Found: C, 62.05; H, 7.30.

[(dpp-Bian)SmBr(dme)]$_2$ (2). The addition of PhCHBr-CHBrPh (0.13 g, 0.4 mmol) to a solution of **1** (0.73 g, 0.8 mmol) in dme (40 mL) caused an immediate change in the color of the solution from red-brown to deep blue. Then the solvent was removed in a vacuum, and the residue was dissolved in benzene (40 mL). Complex **2** (0.32 g, 43%) separated from the filtered and concentrated solution as deep-blue crystals. Mp: 187 °C. ^{1}H NMR (THF-d_8, 400 MHz): δ 7.79 (s, 2 H, CH arom.), 7.63 (s, 4 H, CH arom.), 7.38 (s, 9 H, C_6H_6), 7.29 (s, 2 H, CH arom.), 7.20 (s, 2 H, CH arom.), 7.02 (s, 2 H, CH arom.), 3.46 (s, 4 H, CH_2(dme)), 3.32 (s, 6 H, CH_3(dme)), 1.89 (s, 12 H, CH(CH_3)$_2$), 1.23 (s, 12 H, CH(CH_3)$_2$). UV (293 K, THF): λ 640 nm. IR

(43) (a) Barbier-Baudry, D.; Heiner, S.; Kubicki, M. M.; Vigier, E.; Visseaux, M.; Hafid, A. *Organometallics* **2001**, *20*, 4207–4210. (b) Hou, Z.; Fujita, A.; Yoshimura, T.; Jesorka, A.; Zhang, Y.; Yamazaki, H.; Wakatsuki, Y. *Inorg. Chem.* **1996**, *35*, 7190–7195.

(44) Baranovski, V. I.; Denisova, A. S.; Kuklo, L. I. *THEOCHEM* **2006**, *759*, 111–115.

(Nujol): ν 1946 w, 1910 w, 1850 w, 1798 w, 1709 w, 1671 w, 1611 m, 1580 s, 1431 vs, 1366 m, 1354 w, 1302 s, 1249 s, 1207 w, 1190 s, 1157 w, 1138 w, 1104 s, 1063 s, 1016 s, 982 s, 930 m, 916 m, 889 m, 854 s, 818 s, 799 s, 773 s, 762 s, 701 w, 682 m, 623 m, cm^{-1}. Anal. Calcd for $C_{80}H_{100}Br_2N_4O_4Sm_2 \cdot 3C_6H_6$ (1876.48): C, 62.73; H, 6.34. Found: C, 60.83; H, 6.05.

(dpp-Bian)SmBr$_2$(dme) (3). The addition of PhCHBrCHBrPh (0.26 g, 0.75 mmol) to a solution of **1** (0.69 g, 0.75 mmol) in dme (40 mL) caused an immediate change in the color of the solution from red-brown to cherry red. The crude product left after evaporation of the solvent was crystallized from toluene and afforded complex **3** (0.30 g, 40%) as deep-red crystals. Mp: > 280 °C. IR (Nujol): ν 1914 w, 1853 w, 1791 w, 1718 w, 1667 s, 1650 m, 1640 m, 1611 w, 1592 s, 1523 m, 1429 s, 1363 m, 1326 m, 1303 m, 1278 m, 1249 m, 1190 s, 1160 w, 1113 s, 1052 s, 1020 m, 982 w, 937 m, 926 s, 857 s, 836 s, 817 w, 785 s, 769 w, 762 w, 750 s, 884 w, 622 w cm^{-1}. Anal. Calcd for $C_{40}H_{50}Br_2N_2O_2Sm \cdot {}^1/_2C_7H_8$ (947.06): C, 55.17; H, 5.75. Found: C, 54.59; H, 5.45.

(dpp-Bian)SmI$_2$(THF)$_2$ (4). The addition of dpp-Bian (0.5 g, 1.0 mmol) to a blue solution of SmI_2 in THF (35 mL), prepared in situ from excess samarium metal and I_2 (0.25 g, 1.0 mmol), caused an immediate change in the color of the solution to cherry red. Evaporation of the solvent and crystallization of the remaining solid from diethyl ether yielded complex **4** (0.86 g, 82%) as deep-red prismatic crystals. Mp: 249 °C (dec). IR (Nujol): ν 1663 m, 1638 m, 1612 m, 1579 s, 1490 w, 1433 s, 1362 m, 1346 w, 1324 w, 1282 m, 1253 m, 1223 w, 1180 m, 1161 w, 1149 w, 1111 m, 1088 w, 1055 m, 1041 m, 938 m, 922 m, 833 s, 798 m, 778 s, 755 s, 611 w, 588 w, 536 w cm^{-1}. Anal. Calcd for $C_{44}H_{56}I_2N_2O_2Sm$ (1049.11): C, 50.37; H, 5.38. Found: C, 49.86; H, 5.01.

(dpp-Bian)SmI[SC(S)NMe$_2$](dme) (5). The addition of I_2 (0.1 g, 0.4 mmol) to a solution of **1** (0.75 g, 0.81 mmol) in dme (40 mL), followed by the addition of $[(CH_3)_2NC(S)S]_2$ (0.1 g, 0.4 mmol), caused immediate changes in the color of the solution from red-brown to blue and finally to cherry red. Slow evaporation of the solvent gave compound **5** (0.60 g, 69%) as deep-red crystals. Mp: > 280 °C. IR (Nujol): ν 1609 w, 1588 w, 1519 s, 1433 s, 1421 s, 1378 s, 1364 m, 1317 m, 1295 w, 1255 w, 1225 w, 1184 m, 1054 w, 1035 s, 1013 w, 980 s, 939 m, 888 w, 846 s, 820 m, 803 m, 787 w, 775 m, 764 m, 750 w, 723 w, 793 w, 667 w, 623 w, 604 w, 578 w, 538 w, 513 w, 456 w cm^{-1}. Anal. Calcd for $C_{43}H_{56}IN_3O_2S_2Sm \cdot C_4H_{10}O_2$ (1078.40): C, 52.34; H, 6.17. Found: C, 52.28; H, 6.13.

[(dpp-Bian)SmI(O*t*Bu)(THF)]$_2$ (6). A total of 0.11 mg (1.0 mmol) of *t*BuOK was added to a solution of **4** (prepared in situ from SmI_2 and dpp-Bian as described above) in THF (35 mL). Precipitated KI was filtered off, and the solvent was evaporated from a filtrate. The residual waxy solid was dissolved in hexane (50 mL) at heating (65 °C) and filtered off again. In 24 h at ambient temperature, complex **6** was isolated from hexane as red crystals (0.37 g, 38%). Mp: > 300 °C. IR (Nujol, KBr): ν 1670 m, 1650 m, 1590 m, 1518 s, 1315 m, 1190 m, 1100 m, 1074 m, 1027 m, 991 s, 930 s, 872 m, 850 s, 820 s, 792 s, 760 s, 727 m, 695 m, 666 m, 622 m, 539 m, 511 m, 478 m cm^{-1}. Anal. Calcd for $C_{88}H_{114}I_2N_4O_4Sm_2 \cdot C_6H_{14}$ (1932.50): C, 58.42; H, 6.68. Found: C, 58.30; H, 6.60.

Single-Crystal X-ray Structure Determination of 2−6. The crystallographic data for **2**−**6** were collected on an Oxford Diffraction Xcalibur S Sapphire diffractometer using graphite-monochromated Mo Kα (λ = 0.710 73 Å) radiation at 150 K. The data were corrected for absorption using a semi-empirical absorption correction. The structures were solved by direct methods using *SIR97*[45] (**2**, **5**, and **6**) or *SHELXS-97*[46] (**3** and **4**) and were refined by full-matrix least-squares techniques against F_o^2 by using *SHELXL-97*.[47] All non-hydrogen atoms were refined anisotropically, except those of strongly disordered diisopropyl groups and coordinating THF molecules in **4**. Any attempt to model the highly disordered locations did not achieve a stable and reasonable refinement, except using harsh restraint commands in *SHELX*. The final difference Fourier synthesis showed five significant electron densities aligned in the *a* axis, primarily attributable to the presence of disordered groups or artifacts. In **3**, **5**, and **6**, a significantly disordered solvent molecule was incorporated in the cell. This was treated using the *PLATON* "Squeeze" and "Bypass" functions.[48] The absolute structure in noncentrosymmetric space groups was determined from anomalous dispersion effects and verified according to Flack.[49] Hydrogen atom positions were generated by their idealized geometry and refined using a riding model. Experimental details are given in Table 1. CCDC-746524 (**2**), CCDC-746525 (**3**), CCDC-746526 (**4**), CCDC-746527 (**5**), and CCDC-746528 (**6**) contain the respective supplementary crystallographic data. These data can be obtained free of charge from The Cambridge Crystallographic Data Centre via www.ccdc.cam.ac.uk/data_request/cif.

Acknowledgment. This work was supported by the Russian Foundation for Basic Research (Grant 10-03-00430) and the Alexander von Humboldt Foundation (Partnership Project between the Technical University of Berlin and the G. A. Razuvaev Institute of Organometallic Chemistry, Nizhny Novgorod).

Supporting Information Available: X-ray crystallographic data in CIF format. This material is available free of charge via the Internet at http://pubs.acs.org.

(45) Altomare, A.; Burla, M. C.; Camalli, M.; Cascarano, G. L.; Giacovazzo, C.; Guagliardi, A.; Moliterni, A. G. G.; Polidori, G.; Spagna, R. *J. Appl. Crystallogr.* **1999**, *32*, 115–119.

(46) Sheldrick, G. M. *SHELXS-97 Program for the Solution of Crystal Structures*; Universität Göttingen: Göttingen, Germany, 1990.

(47) Sheldrick, G. M. *SHELXL-97 Program for the Refinement of Crystal Structures*; Universität Göttingen: Göttingen, Germany, 1997.

(48) van der Sluis, P.; Spek, A. L. *Acta Crystallogr., Sect. A* **1990**, *46*, 194–201.

(49) Flack, H. D. *Acta Crystallogr., Sect. A* **1983**, *39*, 876–881.